

Analysis of Wall Locking Phenomena and their Consequences in RFX

V. Antoni, F. Bellina, T. Bolzonella, G. Chitarin, P. Collarin, J.N. DiMarco¹, F. Gnesotto, E. Martines, S. Martini, R. Pasqualotto, S. Peruzzo, R. Piovan, N. Pomaro, G. Seriani, P. Sonato, L. Tramontin, F. Trevisan, M. Valisa

Gruppo di Padova per Ricerche sulla Fusione
Associazioni EURATOM-ENEA-CNR-Università di Padova
Corso Stati Uniti, 4 - 35127 Padova (Italy)

¹Summer Associates/DOE contract 74005ENG36 for Los Alamos

1 Introduction

In many Reversed Field Pinch (RFP) experiments unstable MHD modes are reported to lock in phase and sometimes also to the wall [1,2,3,4]. The role of field errors produced by non-ideal passive and active inductors, besides being theoretically predicted, has been clearly evidenced by experiments. In particular on MST a progressive reduction of field errors coming from various sources enabled an operational window to be found in which no wall locking occurs, with a significant improvement of discharge performance [2].

In RFX all pulses evidence wall locking of MHD modes [5]. This paper first analyses the magnetic boundary conditions in pulses with plasma currents of 500 to 900 kA, giving space distribution and time dependence of the radial field component, which is considered to be crucially involved in mode locking. Then the paper shows how radial fields can affect wall locking position and describes how $m=1$ modes lock to give rise to a stationary helical perturbation. Finally, the consequences of mode locking on parallel energy fluxes at the plasma edge and on heat loads on plasma facing components are discussed.

2 Magnetic boundary conditions in RFX

The main sources of radial field errors in RFX are: the poloidal and toroidal gaps in the shell, the shell portholes, the discrete passive and active conductors, such as the supporting rings of the vacuum vessel and the discrete toroidal field coils.

Poloidal gaps. They are the most important sources of radial field errors [5]. The $m=1$ harmonic is usually the largest one and it significantly affects plasma performance; its amplitude is much higher when locking occurs near one of the two gaps. It has been reduced by means of an active axisymmetric feedback control [6], from typically 50 mT to 10 mT during the flat-top phase, but it is much higher during setting-up, when locking occurs, due to limits in time response of the power amplifiers. Higher order harmonics have been minimised by better programming the field shaping winding currents.

Toroidal field system. Before $t=20$ ms, the radial $m=0$ field B_r is mainly due to induced currents in the vacuum vessel stiffening rings ($n=72$), while the winding contribution to B_r is nearly cancelled by the image currents on the shell. Thereafter, the effect of shell currents becomes significant and B_r assumes the coil periodicity $n=48$. The more the image currents penetrate the shell thickness, the larger their effect is on B_r ; therefore, this contribution to B_r

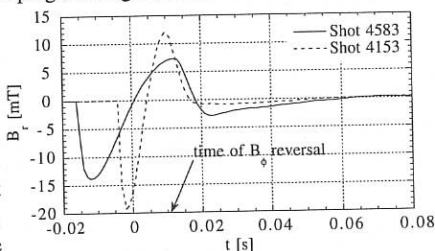


Fig. 1 Evolution of the radial field due to the toroidal field system, computed at first wall.

depends on the time derivative of the winding currents. In fig.1 the time evolution of B_r at the first wall is shown; the dashed waveform refers to a two times faster variation of the toroidal field with respect to the other one.

Equatorial portholes and gap. An analytical model based on measurements by probes placed on the 12 pumping ports is used to calculate the radial field at the plasma edge

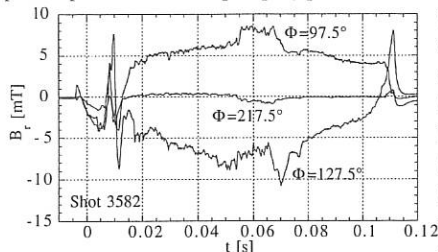


Fig.2 Radial field at plasma edge at Equatorial Portholes.

due to the equatorial holes and to the outer toroidal gap of the shell. In fig.2 B_r at the graphite is shown as a function of time for a typical 530 kA pulse where the locking position is between the ports at $\phi=97.5^\circ$ and $\phi=127.5^\circ$. After fast fluctuations of B_r during the reversal phase, a stationary perturbation becomes evident around $t=15$ ms; for comparison, B_r is also given far from the locking position ($\phi=217.5^\circ$).

Vertical portholes. The radial magnetic field penetration across these portholes, that are not crossed by shell gaps, was studied with a set of two saddle coils placed on the external shell surface around two vertical portholes on the top and bottom sides of the torus. A $m=1$ radial field is detected only when the modes lock near to the probe; it has a typical growth time constant of about 100 ms and the maximum B_r is $3+4$ mT. Since the $m=1$ mode amplitude forced by locking has a much shorter rise time, it is evident that the shell acts as a low-pass shield at these holes, unlike at the equatorial ones.

3 Relationship between field error and mode locking

In normal operation, modes tend to lock preferentially near one of the two shell poloidal gaps [5]. Modes were induced to lock in a predetermined position by reducing to zero the current in 1/12 of the toroidal field winding, at the expense of a substantial confinement degradation. On the other hand, a fairly uniform distribution of locking positions has been obtained by increasing approximately by 50% the current flowing after reversal in the toroidal field coils located over both poloidal gaps: this causes application of a higher toroidal field reversal in the gap regions. A possible explanation of why the current increase affects locking position is found in fig.3, where the $m=0$ B_r measured at the poloidal gaps by saddle coils

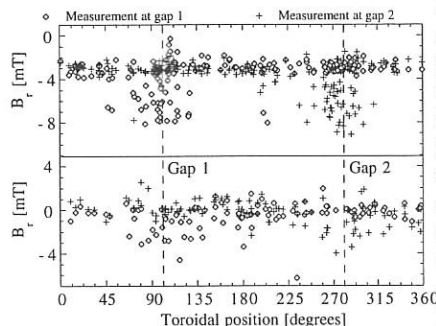


Fig.3: Radial field measured at poloidal gaps, without (above) and with (below) higher reversal applied.

located on the shell inner surface is plotted as a function of locking position, both in standard operation (above) and with the increased field (below), at $t=20$ ms. A radial field of ≈ 3 mT entering through the poloidal gaps is found in standard operation regardless of the locking position; when modes lock at one gap, it is strongly amplified. Due to asymmetry in the electrical connections of the coils with respect to the gaps, the increased toroidal field at the gaps produces a B_r opposite in sign to the one normally found in this region, so that the two tend to cancel out. In this case even the

B_r created when modes lock at one gap is lower than before. These results confirm that radial fields are important as seeds for locking modes to the wall.

4 Space and time analysis of locked modes

Locked modes in RFX are internally resonant with $m=1$, $n=7\div 15$, with $n=8$ usually predominant [5]. The localised perturbation on the toroidal field component is typically 10% of the poloidal field at the wall, corresponding to a spatial RMS value of $2\div 3\%$.

The plasma column deformation due to mode locking has been studied with a poloidal array of pick-up coils located on the shell inner surface, far from the poloidal gaps, in a set of discharges where locking took place near to this array. The result is that mode locking causes a helical distortion of the plasma column (kink) with a pitch of $\approx 1/9$ of the toroidal circumference. The distortion is significant over a toroidal length of ≈ 45 degrees, and its amplitude is equivalent to a plasma column shift of ≈ 1 cm from the equilibrium position.

The modes making up the localised perturbation are already locked to the wall at the beginning of the RFP phase. During start-up, due to the decrease of the safety factor q ,

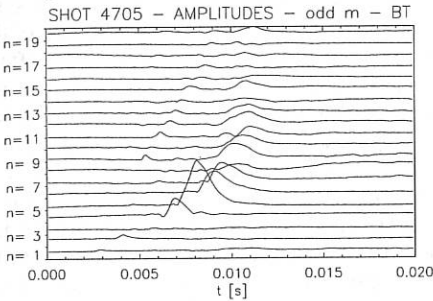


Fig.4 Evolution of modes with odd m during start-up.

reached by low n modes during start-up are roughly proportional to plasma current and tend to be lower when toroidal field reverses faster.

5 Effects of mode locking on heat and particle fluxes at the wall

Energy fluxes parallel to the magnetic field in the outer region of the RFP plasma are characterised by a strong asymmetry between the electron and the ion drift sides, attributed to superthermal electrons. In RFX typical values of this asymmetry, defined as the ratio between the energy fluxes collected on the two sides, are of the order of $2\div 5$ [7]. A detailed analysis of data coming from shots where modes are locked near the calorimetric probes shows that the presence of locked modes causes an inversion of the asymmetry (fig.5).

Mode locking produces helical footprints on the first wall with local enhancement of both power load and impurity influxes, documented by four CCD-TV cameras equipped with interference filters. Fig.6 shows a tangential view from an equatorial port; comparison with magnetic probe data shows that the two poloidal bright stripes correspond to the regions where the magnetic surfaces intercept the wall. Both stripes follow a helical structure with a pitch of $1/14$ of the toroidal circumference. The two regions of interaction differ in terms of power flow direction, the left stripe being heated preferentially from top to bottom (electron drift) while the other along the ion drift. The interaction is concentrated on the edges of the tiles and on the caps protecting the tile clamping keys. Surface temperatures exceeding 2500 °C have been estimated on some hot spots and associated to carbon blooms which increase

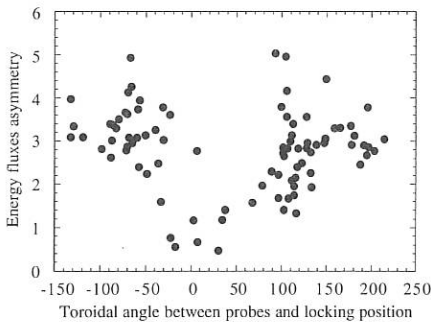


Fig.5 Asymmetry as a function of locking position.

effective Z from the typical values of 2 to 4+5, thus dramatically affecting discharge performance. Such temperature values require power loads of the order of 80+150 MW/m². The area subject to these power flows is estimated to be less than a few thousandths of the total area (36 m²), so that the power lost by transport in the region of enhanced interaction is up to 10+20% of the ohmic input, as previously estimated [5].

Inspection of the first wall tiles and of the vessel inner surface has shown that the regions close to the poloidal gaps present the highest concentration of plasma-wall interaction phenomena: on the lower side of the torus, thermal erosion of the tile edges facing the electron drift side and melting of the vessel

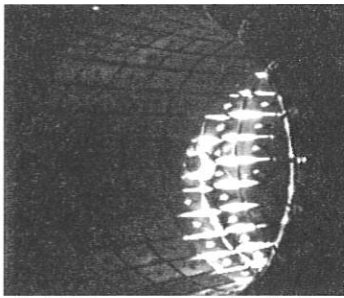


Fig.6 CCD camera observation of locking.

metal surface between the two poloidal rows of tiles adjacent to the gap; on the upper side, a more diffused interaction, also in the toroidal direction, both on tiles and metal wall. Melting of the metal wall on the lower side suggests the presence of large radial magnetic fields. The tiles extracted from the lower side of the torus show the presence of an electron flow through them from the plasma to the vessel. This current, of the order of some kA/tile, is mainly concentrated in one of the two poloidal tile rows adjacent to the poloidal gap. The electron current seems to come out from a larger area on the upper side of the torus.

6 Conclusions

A detailed survey of the radial field errors in RFX has been carried out, leading to identify the poloidal gaps as the main source. Evidence has been found of correlations between field errors and wall locking of MHD modes. Wall locking produces large concentrations of electron and energy fluxes on the first wall, leading to significant erosion of plasma facing materials. Enhanced plasma-wall interaction due to locking causes degradation in confinement, at least by direct losses to the wall and by enhanced impurity production. With the aim of suppressing wall locking, provisions are being taken to reduce the field error level: closure of the outer equatorial gap, closure of one of the two poloidal gaps, fast active control of radial field at the remaining poloidal gap.

References

- [1] R. J. LaHaye et al., Phys. Fluids **27**, 2576 (1984).
- [2] A. F. Almagri et al., Phys. Fluids B **4**, 4080 (1992).
- [3] P. R. Brunzell et al., Phys. Fluids B **5**, 885 (1993).
- [4] S. Mazur, Phys. Plasmas **1**, 3356 (1994).
- [5] A. Buffa et al., 21st EPS Conference (Montpellier, 1994), part I, p. 458.
- [6] P. Bettini et al., Improved RFX Operation by Active Magnetic Field Control, this Conf.
- [7] V. Antoni et al., 21st EPS Conference (Montpellier, 1994), part II, p. 695.